Raman Fiber Laser–Based Amplification in Telecommunications

Mingming Tan

Additional information is available at the end of the chapter

Abstract

The chapter demonstrates a detailed study of Raman fiber laser (RFL)-based amplification techniques and their applications in long-haul/unrepeatered coherent transmission systems. RFL-based amplification techniques are investigated from signal/noise power distributions, relative intensity noise (RIN), and fiber laser mode structures. RFL-based amplification techniques can be divided into two categories according to the fiber laser generation mechanism: cavity Raman fiber laser with two fiber Bragg gratings (FBGs) and random distributed feedback (DFB) Raman fiber laser using one FBG. In addition, in cavity fiber laser–based amplification, reducing the reflectivity near the input helps mitigate the signal RIN, thanks to the reduced efficiency of the Stokes shift from the second-order pump. To evaluate the transmission performance, different RFL-based amplifiers were optimized in long-haul coherent transmission systems. Cavity fiber laser–based amplifier introduces >4.15 dB Q factor penalty, because the signal RIN is transferred from the second-order pump. However, random DFB fiber laser–based amplifier prevents the RIN transfer and therefore enables bidirectional second-order pumping, which gives the longest transmission distance up to 7915 km. In addition, using random DFB laser-based amplification achieves the distance of >350 km single mode fiber in unrepeatered DP-QPSK transmission.

Keywords: Raman amplification, Raman fiber laser, coherent transmission, random fiber laser, cavity fiber laser

1. Introduction

In this chapter, we focus on the novel Raman fiber laser (RFL)-based amplification techniques enabled by second-order pumping and fiber Bragg gratings (FBGs) at first-order pumping

wavelengths [1], which is different from the conventional first-order or dual-order pumping schemes [2–4]. In first-order distributed Raman amplification, the signal is amplified by multiple first-order depolarized laser diodes to achieve flat gain profile. However, the signal gain can only occur near the fiber output, resulting in larger signal power profile and higher amplifier noise figure, which becomes the limiting factor of its performance in long-haul or unrepeatered transmission systems [2, 4]. In conventional dual-order Raman amplification, more uniform signal power distribution can be achieved, thanks to the Raman gain that occurs in the middle of the fiber. However, both first-order and second-order pump sources are also required. Particularly, to minimize the amplifier noise figure, the first-order pump power should be very small to enable higher second-order pump power, which requires multiple current and temperature controllers for the pump lasers [5]. Thus, the Raman fiber laser–based amplification reduces the high cost of dual-order pumping and improves the amplifier performance in comparison with first-order pumping, as it uses only second-order pumping with passive FBGs [1, 5].

In general, second-order RFL-based amplification is a distributed Raman amplification scheme, requiring depolarized second-order pumps (~1360 nm assuming the amplified signal is in C band, thanks to the two Stokes shift) and passive FBGs to generate first-order ultra-long Raman fiber laser when the transmission fiber is used as the gain medium. The induced Raman fiber laser together with the residual second-order pump is to amplify the signal in C and/or L band [6, 7]. However, due to different generation mechanisms of induced Raman fiber laser, there are two fiber laser regimes [8]. The first scheme is cavity fiber laser, in other words, Fabry-Perot cavity, where the transmission fiber between two end reflectors forms an ultra-long fiber laser cavity [9, 10]. This can be done with two high reflectivity FBGs or alternatively an FBG with weak Fresnel reflection [11, 12]. Random distributed feedback (DFB) Raman fiber laser is the other laser regime [13]. This is generated because the lasing threshold is overcome in the cavity formed by a distributed feedback (fiber Rayleigh scattering) and high reflective FBG [5, 14, 15].

RFL-based amplification schemes have different impacts on the coherent transmission systems, depending on the pumping schemes. Cavity fiber laser–based amplification can introduce a significant Q factor penalty, limiting the maximum reach to only 1500 km [2, 3, 8, 16], which means that that using forward (FW)-propagated pumping introduced a Q factor penalty, regardless of the reduction in the amplifier noise figure. However, random fiber laser–based amplification mitigates the signal relative intensity noise (RIN), reveals the benefit of the lower noise figure brought by FW-pumping, and effectively extends the maximum reach of the long-haul transmission system [5]. Such random fiber laser–based amplification technique can be applied in unrepeatered transmission systems and achieve a record transmission distance of over 350 km standard single mode fiber (SSMF) using 22 × 100 Gbits DP-QPSK WDM transmitter [17].

RFL-based amplification techniques are characterized from different perspectives, including signal/noise power distributions, relative intensity noise (RIN), and the mode structures of fiber laser. These results help give a better understanding of RFL-based amplification and also support the long-haul and unrepeatered coherent transmission performances demonstrated in this chapter.

2. Raman fiber laser–based amplification

2.1. Cavity Raman fiber laser amplification

2.1.1. Experimental setup

Figure 1 shows the schematic diagram of cavity fiber laser–based amplification using two FBGs. Two high reflectivity (>~95%) FBGs at 1455 nm with 3 dB bandwidths of ~0.5 nm were used at both ends of an 83 km SSMF. When the pump power of depolarized continuous wave second-order pumps at 1366 nm was high enough to overcome the lasing threshold, an ultra-long Fabry-Perot cavity (83 km was the cavity length) fiber laser was generated at 1455 nm [1, 5, 14, 15]. Therefore, the generated first-order fiber laser at 1455 nm and the second-order pump at 1366 nm amplified the signals in the C band [7].

The FW pump and BW pump powers used in the experiment were demonstrated in (**Figure 2**) and only used to compensate the ~16.5 dB loss from the 83.32 km fiber. The FW pump power ratio means the percentage of the FW pump power out of total pump power.

2.1.2. Signal and noise power distributions along the fiber

Signal power distributions along the transmission fiber with different pump powers were measured at 1545.32 nm using a modified optical time-domain reflectometer (OTDR) setup [6]. The OTDR instrument was used to monitor the signal power traces along the fiber. The built-in pulsed Fabry-Perot semiconductor laser at 1550 nm was transferred into the RF pulses which modulated an externally tunable laser through an acoustic optical modulator (AOM). The pulsed tunable laser was then transmitted into the fiber under test (Raman amplified), and the reflections were fed into the OTDR instrument. In this way, the signal power profile along the Raman-amplified fiber span was acquired.

Figure 3 shows both the experimental (solid) and simulated (dotted) signal power profiles [8, 18, 19]. The simulations use a set of equations to describe the power evolution [1]. The signal power profiles were the mutual effect of second-order pump power profiles at 1366 nm and first-order Raman fiber laser power profiles at 1455 nm [8]. For different pump-power combinations, signal power variation (SPV) was calculated as the difference between the maximum and minimum power value along the span, which was used as a metric to compare different pumping schemes. The lowest SPV of ~1.6 dB (+/−0.8 dB) over 83 km SSMF was done by
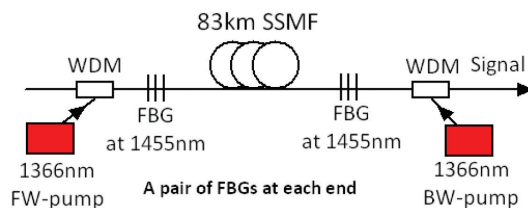
Figure 1. Cavity fiber laser–based amplification with two FBGs.

FW-pump power (dBm)	BW-pump power (dEm)	FW-pump power ratio
0.0	31.2	0.0%
25.5	29.7	27.6%
26.0	29.6	30.4%
26.5	29.4	33.9%
27.0	29.2	37.6%
27.5	29.0	41.4%
28.0	28.6	46.4%

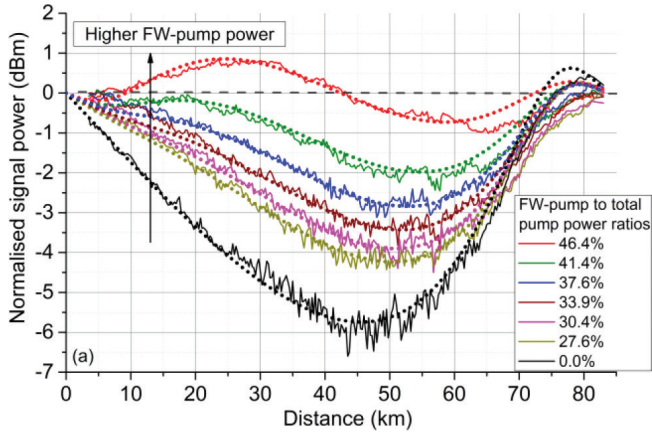**Figure 2.** The pump power used in the cavity fiber laser–based amplification.

Figure 3. Measured (solid) and simulated (dotted) signal power distributions.

bidirectional pumping with the similar pump powers from both directions. The SPV was increased to ~5.6 dB using BW-pumping only. This means that the second-order FW-pumping reduced the power variation and increased the average signal power relatively, so the noise figure of a distributed Raman amplifier was reduced [4]. **Figure 4** shows the simulated noise power profiles. Compared with BW-pumping only, the noise power was decreased up to ~4 dB using bidirectional pumping. Considering the ASE noise only, the more the FW pump power, the less the ASE noise (the lower the amplifier noise figure). However, when the distributed Raman amplification is evaluated in the long-haul transmission system, the optimum signal launch power depends on the best trade-off between the ASE noise and the nonlinearity (if the RIN-induced penalty from the forward propagated pump is not taken into account). This means that the flat signal power profiles (the smallest power variation) are the key to achieve the best transmission performance using high-order symmetric bidirectional pumping instead of FW-pumping only [5].

2.1.3. Relative intensity noise

Relative intensity noise (RIN) is essentially the intensity variations from the pump source [16]. As the process of the Raman gain is extremely fast, the noise from the pump can affect the
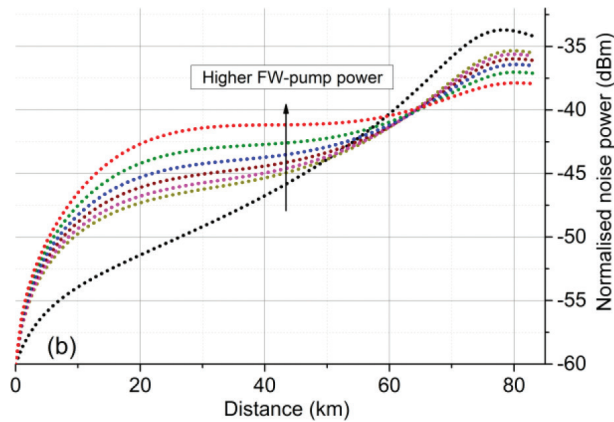
Figure 4. Simulated noise power distributions.

signal. When the pump and the signal travel in the same directions (usually called FW-pumping or co-pumping), the pump noise is more likely to transfer to the signal [3, 16, 20]. When the pump and the signal travel in the reverse, as the pump noise is attenuated and averaged by the transmission fiber [3, 21], BW-pumping is more tolerant to the RIN. FW-pumping can improve the noise figure but increase the signal RIN at the same time. For long-haul transmission, as the RIN is accumulated over the number of spans, the RIN penalty would be very severe. The schematic design of the RIN measurement is illustrated in [8]. The setup for the RIN measurement was based on an ultra-low-noise receiver and an electrical spectrum analyzer (ESA) ranging from 1 up to 160 MHz. The measured RIN of the second-order pump at 1366 nm is ~−120 dB/Hz, which is likely to be the lowest on the market for fiber laser–based pumps. The RIN of the output signal at 1545.32 nm was measured after one span from a CW low RIN (~−145 dB/Hz RIN) tunable laser source, and the FW-propagated Fabry-Perot fiber laser through a 5% splitter was measured.

Figure 5 shows the measured signal RIN in cavity fiber laser–based amplifier using different pump power combinations. When the FW pump power ratio was increased to 46.4%, the signal RIN was 18 dB higher, compared with BW-pumping only. The RIN increase was 9 dB using a 27.6% FW-pumping ratio. **Figure 6** shows the RIN for the first-order-induced fiber laser. The fiber laser RIN was similar for all the pump powers used, except that the fiber laser RIN with BW-pumping only was lower within the range of below 40 MHz. Overall, there were significant differences in RIN between the BW-pumping scheme and all the other schemes using FW-pumping.

2.1.4. Fiber laser mode structures

Figure 7 shows the measured intra-cavity electrical spectra of the FW-propagated fiber laser at 1455 nm for different FW pump powers. Note that the traces in **Figure 7** are deliberately offset to aid the comparison. It indicates that there were two different fiber lasing regimes. Using FW-pumping, a ~1.2 kHz mode spacing was acquired which corresponded to an 83 km
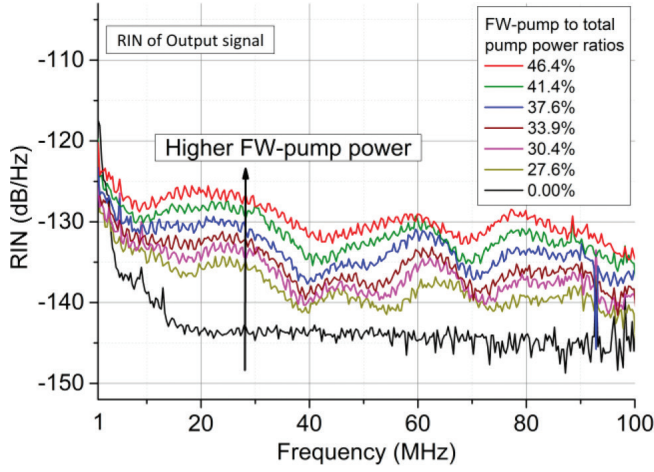
Figure 5. RIN of the output signal using different pump powers in cavity fiber laser–based amplification technique.
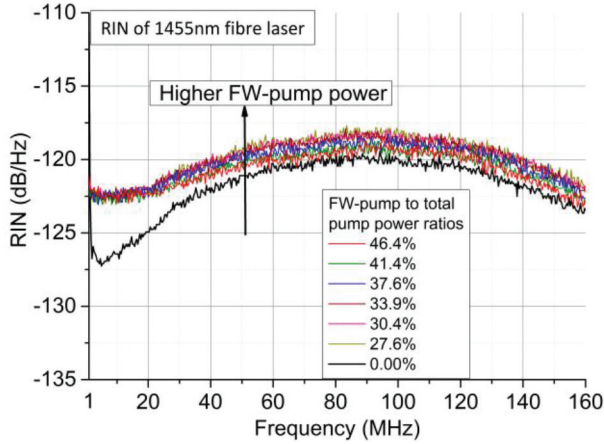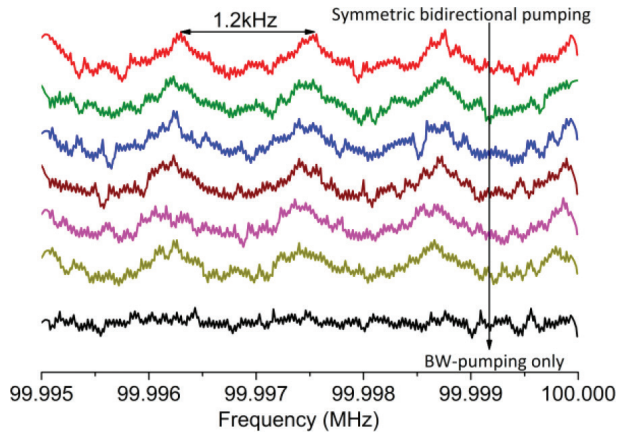

Figure 6. RIN of the induced fiber laser using different pump powers in cavity fiber laser–based amplification technique.

Fabry-Perot cavity. This mode spacing did not depend on the FW pump power used, because it was determined by the cavity length and the refractive index [10], as demonstrated in Eq. (1). Δv is the mode spacing, c is the speed of the light, n is the fiber refractive index, and L is the length of the cavity.

$$\Delta v = \frac{c}{2nL} \tag{1}$$

No mode structure ("modeless" fiber laser) can be seen in BW-pumping only. This was because although a high reflectivity FBG was placed on one side of the cavity, distributed fiber Rayleigh scattering formed on the other side of the cavity, which generated a half-open

Figure 7. Mode structures of the induced fiber laser using different pump powers in cavity fiber laser–based amplification technique.

fiber laser cavity [15, 22]. Thus, the cavity length of this fiber laser was not fixed due to the randomly distributed Rayleigh backscattering from the fiber [22]. Overall, these results show that with closed cavity with two FBGs, a random DFB fiber laser can be still achieved, which is different from the usual Fabry-Perot fiber laser with bidirectional pumping.

Figure 7 shows that in the fiber span of 83 km, using bidirectional pumping forms a Fabry-Perot cavity fiber laser. On the other hand, using BW-pumping only forms a random DFB fiber laser. However, when the fiber in between FBGs is too long (i.e. >270 km) [10], even with bidirectional pumping, the induced fiber laser is still random DFB fiber laser. This is because due to the high fiber attenuation, the pumps are "isolated" from each other, not powerful enough to reach the FBG on the other side. Instead, similar to the BW-pumping only over 83 km, the fiber Rayleigh backscattering reflects the pump and therefore generates a random fiber laser. Using bidirectional pumping over a very long fiber span generates two separate random fiber lasers at the input and the output [17]. This can be used in unrepeatered transmission systems.

2.2. Random distributed feedback Raman fiber laser–based amplification

2.2.1. Experimental setup

The reflectivity near the input section was close to zero (measured result of 0.04%), achieved by replacing it with an angled connector instead. The schematic diagram of such an amplifier is illustrated in **Figure 8**. The FW pump and BW pump powers are demonstrated in **Figure 9**. Note that the pump powers were only to compensate the loss of 83 km SSMF.

2.2.2. Signal and noise power distributions along the fiber

The signal and noise power distributions along the fiber were shown experimentally (solid line) and theoretically (dotted line) in **Figure 10** [5]. Using the BW-pumping only, the SPV was
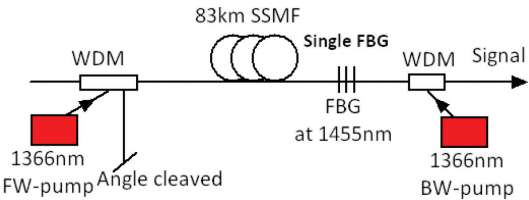
Figure 8. Random fiber laser–based amplification with one FBG.

FW-pump (dBm)	BW-pump (dBm)	FW-pump power ratio
0	31	0%
27.5	30.6	33.1%
28.7	30.5	39.7%
29.7	30.4	45.6%
30.3	30.4	49.7%

Figure 9. The pump power used in random fiber laser–based amplification.
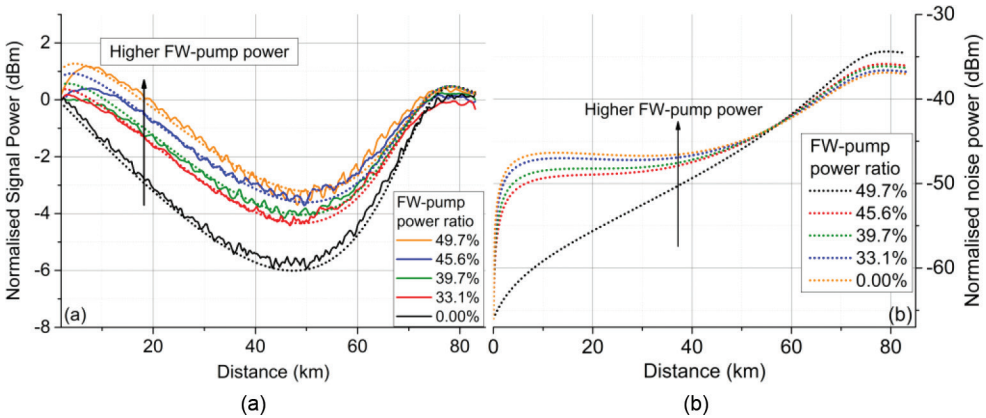

Figure 10. Measured (solid) and simulated (dotted) signal (a) and noise power profiles (b) using random fiber laser–based amplification scheme.

the highest (~6 dB). Using 45.6 or 39.7% FW-pumping ratios, the lowest SPV was reduced to just below 4 dB. However, for the FW pump power ratio of 45.6%, a rapid power increase was seen within the first 10 km near the input end. This was particularly undesired for long-haul transmission systems because this was limited to the maximum signal launch power in order to avoid the Kerr nonlinear impairment [23].

In addition, random DFB fiber laser–based amplification is a good candidate for long-haul transmission system using mid-link optical phase conjugation (OPC) to combat the nonlinearity,
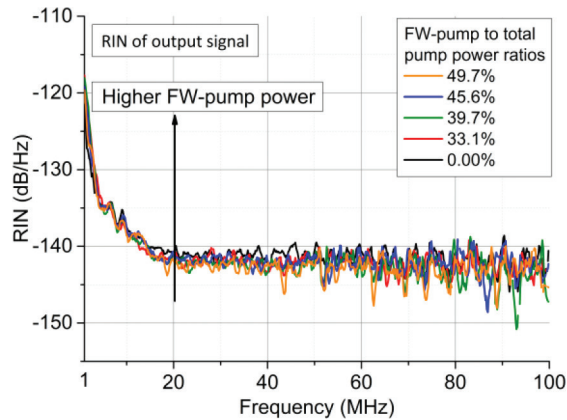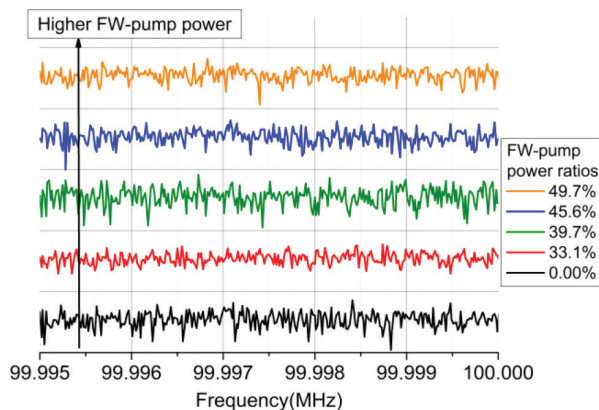
Figure 11. Signal RIN using different pump powers in random fiber laser–based amplification technique.

given the good signal power symmetry of the link [24, 25]. As illustrated in [24], more than 97% symmetry level can be achieved using this amplification technique over 62 km SMF. There are several generation mechanisms of random DFB fiber lasers, but here only the half-opened mechanism is discussed due to the highest Raman gain efficiency [26].

2.2.3. Relative intensity noise

The RIN of the signal at the output end was shown in **Figure 11**. The signal RIN remained the same with the FW pump power over the whole frequency range. This means that the transmission performance can only depend on the balance between the ASE noise and nonlinearity without the RIN-induced penalty being considered [23].

Figure 12. Mode structures of the induced fiber laser using different pump powers in random fiber laser–based amplification technique.

2.2.4. Fiber laser mode structure

Figure 12 shows the mode structure of induced fiber laser with different pump powers. No mode was observed using BW-pumping only or bidirectional pumping, which confirms that it was random DFB fiber laser [8, 15]. The fiber laser was generated due to the resonant mode overcoming the lasing threshold in a distributed cavity formed by the fiber Rayleigh scattering and an FBG.

3. Raman fiber laser–based amplification in telecommunications

3.1. The application in long-haul coherent transmission system

To evaluate different RFL-based amplification schemes, a long-haul recirculating loop experiment was conducted using the setup demonstrated in **Figure 13**. The test signals consisted of 10,120 Gb/s DP-QPSK channels with 100 GHz spacing, while a 100 kHz linewidth tunable laser was used as the "channel under test." The multiplexed signals were QPSK modulated with normal and inverse $2^{31}-1$ PRBS patterns at 30 Gb/s with a relative delay of 18 bits between I (in-phase) and Q (quadrature). A polarization multiplexer with a delay of 300 bits between the two polarization states gave the resultant 10 × 120 Gb/s DP-QPSK signals [24]. The transmission span in the recirculating loop was 17.6 dB loss in total, including 16.5 dB from 83.32 km SSMF and 1.1 dB from pump-signal combiners. The loop specific loss was ~12 dB from the AOM, 3 dB coupler, gain flattening filter (GFF), and the passive components from the Raman amplified span. An EDFA was used to compensate the loop loss. The receiver was a standard coherent detection setup and digital signal processing (DSP) was used offline with standard algorithms. Q factors were calculated from bit-wise error rates.
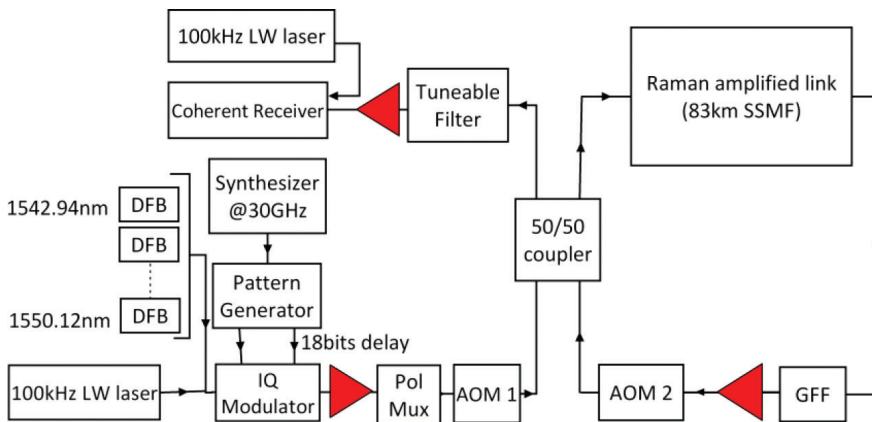

Figure 13. Schematic diagram of long-haul repeatered transmission systems.

As cavity fiber laser–based amplification in **Figure 1** was used in the long-haul transmission, as shown in **Figure 14(a)**; the Q factor at 1666 km was 13.1 dB (BW-pumping only) but decreased to 9 dB (symmetric bidirectional pumping). Using higher FW pump power reduced the Q factor due to the RIN penalty, regardless of the noise figure reduction [8]. The optimum launch power was reduced when the FW pump power was increased. This was because the flatter signal power profile resulted in a higher averaged signal power and therefore the optimum signal launch power was decreased to avoid the Kerr nonlinearity. The degradation in Q factor occurred in all the launch power levels, which indicates that it was not because of the nonlinearity. However, in random fiber laser–based amplification scheme (**Figure 8**) as the FBG near the input was removed, the Q factor at 3333 km (**Figure 14(b)**) with FW pump power ratio of 33% was 0.6 dB better than BW-pumping only, and even using ~50% FW pump power ratio had a similar Q factor to BW-pumping only. This means that using this scheme, the RIN penalty introduced by FW-pumping was minimized, which indicates that the uniform signal power distribution led to effective performance improvement in long-haul transmission systems.

Figure 15 shows the Q factors versus transmission distances using both the amplification schemes. Using random fiber laser–based amplification had similar or better transmission performance (up to 7915 km maximum reach) than the BW-pumping-only scheme, but using cavity fiber laser–based scheme had a significant penalty. An important application of this RIN penalty-free random fiber laser–based amplification scheme was in the nonlinearity mitigation using mid-link OPC because using the scheme had a very symmetrical signal power profile and could maximize the benefit of nonlinearity compensation using mid-link OPC. The details of this work can be found in [24, 25].

3.2. The application in unrepeatered coherent transmission system

In unrepeatered transmissions, distributed Raman amplification offers enhanced noise performance leading to higher OSNR, compared with EDFA [16, 27]. By using higher order distributed
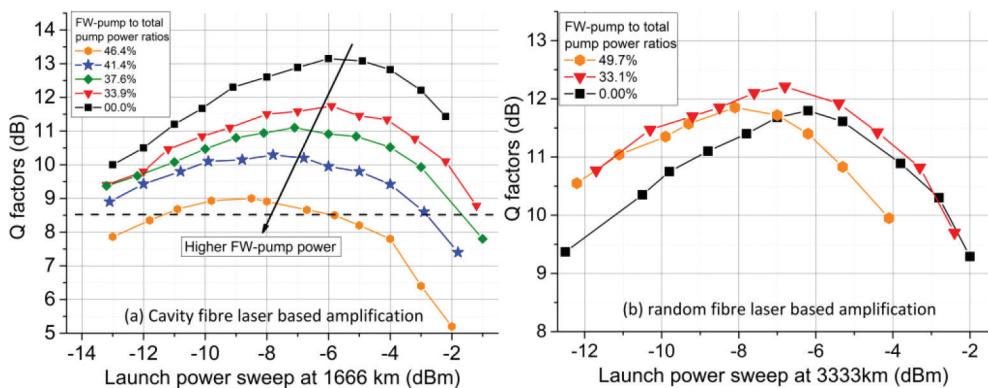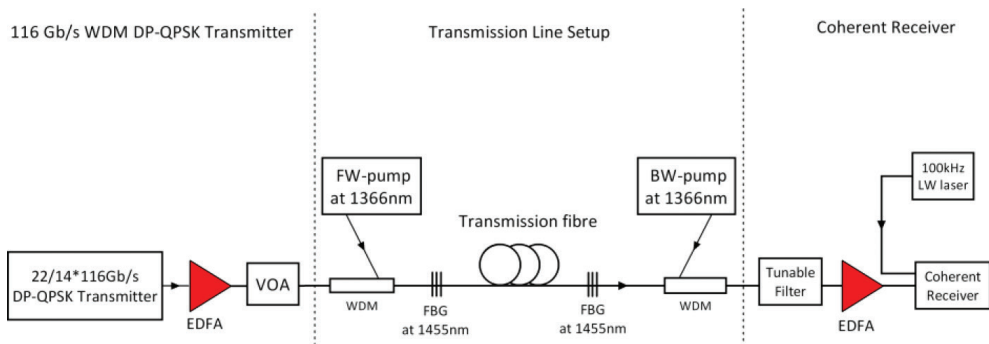

Figure 14. (a) Q factors versus signal launch power using cavity fiber laser–based amplification and (b) Q factors versus signal launch power using random fiber laser–based amplification.
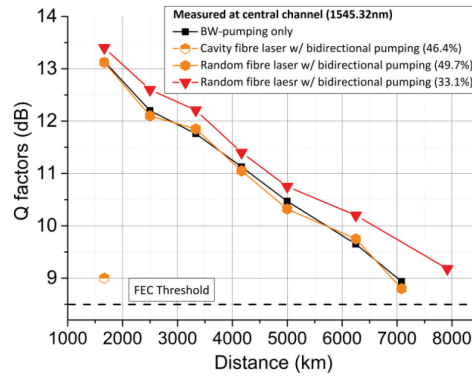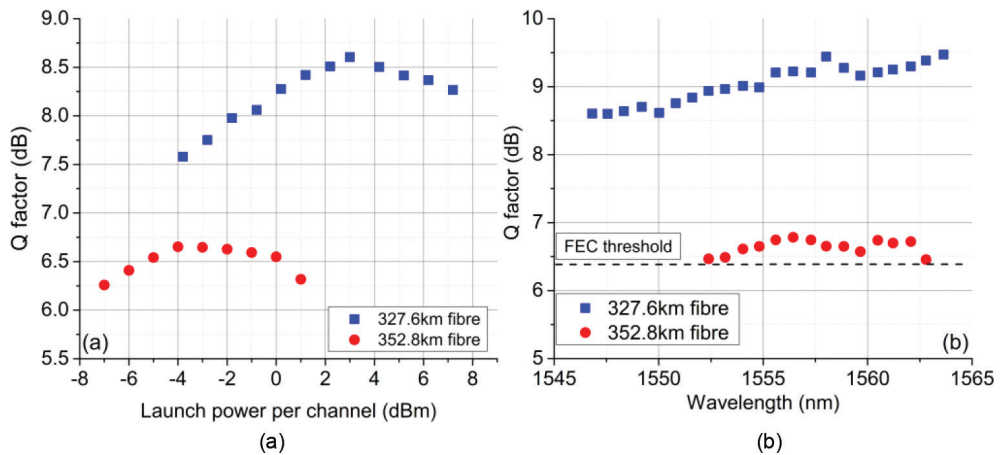
Figure 15. Q factors versus signal launch power using BW-pumping only, cavity fiber laser–based amplification scheme, and random fiber laser–based amplification scheme.

Raman amplifications, the signal power variation can be reduced leading to highly uniform signal power profiles, better trade-offs between ASE noise and nonlinearity, and better transmission performance. Here, based on the RFL-based amplification, the transmission performance using 100G DP-QPSK WDM signals over 352.8 km SMF has been shown without using remote optically pumped amplifier (ROPA) or any specialty fiber [17].

Figure 16 shows the schematic diagram of the unrepeatered transmission system using DP-QPSK WDM signals and random fiber laser–based amplification technique. An important difference of RFL-based amplifier in unrepeatered and repeatered systems is that due to the fiber length of the unrepeatered system (i.e. 300 km), the generated Raman fiber laser at 1455 nm was actually two separate random DFB fiber lasers located near each side of the span and had no interaction with each other [5, 17]. **Figure 17(a)** shows the Q factor versus signal launch power per channel, and **Figure 17(b)** shows the Q factors of all the measured channels at 327.6 and 352.8 km. At 327.6 km, the maximum number of channels was limited to the number of lasers we had. At 352.8 km, 14 channels were transmitted at the FEC threshold

Figure 16. A schematic diagram of random fiber laser–based amplification scheme in unrepeatered transmission.

Figure 17. (a) Q factors versus launch power per channel at 327.6 and 352.8 km and (b) Q factors of all the measured channels at 327.6 and 352.8 km.

of 6.4 dB. This was achieved without ROPA and low-loss fiber, which indicates that our proposed setup can be used to readily upgrade the existing SSMF legacy link without the installation of the new fiber. In addition, our proposed setup is compatible with ROPA by adding the seed pump at 1480 nm, which can simultaneously improve the transmission distance and the amplification bandwidth [28-30].

4. Conclusion

In conclusion, Raman fiber laser–based amplification techniques have been characterized as standalone amplifiers, and its performances have been analyzed and optimized in long-haul repeatered and unrepeatered coherent transmission systems. Based on random DFB fiber laser–based Raman amplification, the signal RIN can be successfully mitigated, and bidirectional second-order pumping would not suffer from the RIN penalty. Thus, it provides the best trade-off between ASE noise and nonlinearity and therefore offers the best transmission performance. The scheme is highly flexible and the signal power distributions can be adjusted to meet specific link requirements. This scheme is potentially to be highly effective to compensate the nonlinear impairment and enhance the transmission distance using different nonlinearity compensation techniques, that is, mid-link optical phase conjugation and nonlinear Fourier transform-based transmitter.

Acknowledgements

Author details

Mingming Tan

Address all correspondence to: m.tan1@aston.ac.uk

Aston Institute of Photonic Technologies, Aston University, Birmingham, UK

References

[1] Ania-Castañón JD. Quasi-lossless transmission using second-order Raman amplification and fiber Bragg gratings. Optics Express. 2004;**12**:4372-4377

[2] Bromage J. Raman amplification for fiber communications systems. Journal of Lightwave Technology. 2004;**22**:79-93

[3] Fludger CRS, Handerek V, Mears RJ. Pump to signal RIN transfer in Raman fiber amplifiers. Journal of Lightwave Technology. 2001;**19**:1140-1148

[4] Bouteiller J-C, Brar K, Headley C. Quasi-constant signal power transmission. In: ECOC. 2002. pp. 1-2

[5] Tan M, Rosa P, Le ST, Md A, Iqbal IDP, Harper P. Transmission performance improvement using random DFB laser based Raman amplification and bidirectional second-order pumping. Optics Express. 2016;**24**:2215-2221

[6] Ania-Castañón JD, Karalekas V, Harper P, Turitsyn SK. Simultaneous spatial and spectral transparency in ultralong fiber lasers. Physics Review Letters. 2008;**101**:123903

[7] Ellingham TJ, Ania-Castañón JD, Ibbotson R, Chen X, Zhang L, Turitsyn SK. Quasi-lossless optical links for broad-band transmission and data processing. IEEE Photonics Technology Letters. 2006;**18**(1):268-270

[8] Tan M, Rosa P, Le ST, Phillips ID, Harper P. Evaluation of 100G DP-QPSK long-haul transmission performance using second order co-pumped Raman laser based amplification. Optics Express. 2015;**23**:22181-22189

[9] Ania-Castañón JD, Ellingham TJ, Ibbotson R, Chen X, Zhang L, Turitsyn SK. Ultralong Raman fiber lasers as virtually lossless optical media. Physical Review Letters. 2006; **96**(2):023902

[10] Turitsyn SK, Ania-Castañón JD, Babin SA, Karalekas V, Harper P, Churkin D, Kablukov SI, ElTaher AE, Podivilov EV, Mezentsev VK. 270-km ultralong Raman fiber laser. Physical Review Letters. 2009;**103**(13):133901

[11] Gallazzi F, Rizzelli G, Md A, Iqbal MT, Harper P, Ania-Castañón JD. Performance optimization in ultra-long Raman laser amplified 10×30 GBaud DP-QPSK transmission: Balancing RIN and ASE noise. Optics Express. 2017;**25**:21454-21459

[12] Rizzelli G, Iqbal MA, Gallazzi F, Rosa P, Tan M, Ania-Castañón JD, Krzczanowicz L, Corredera P, Phillips I, Forysiak W, Harper P. Impact of input FBG reflectivity and forward pump power on RIN transfer in ultralong Raman laser amplifiers. Optics Express. 2016;**24**:29170-29175

[13] Turitsyn SK, Babin SA, El-Taher AE, Harper P, Churkin DV, Kablukov SI, Ania-Castañón JD, Karalekas V, Podivilov EV. Random distributed feedback fibre laser. Nature Photonics. 2010;**4**:231-235

[14] Papernyi SB, Karpov VI, Clements WRL. Third-order cascaded Raman amplification. In: Optical Fiber Communications Conference (Optical Society of America, 2002), Paper FB4

[15] Zhang WL, Rao YJ, Zhu JM, Yang ZX, Wang ZN, Jia XH. Low threshold 2nd-order random lasing of a fiber laser with a half-opened cavity. Optics Express. 2012;**20**:14400-14405

[16] Pelouch WS. Raman amplification: An enabling technology for high-capacity, long-haul transmission. In: OFC 2015, Paper. W1C.1

[17] Rosa P, Tan M, Le ST, Philips ID, Ania-Castañon JD, Sygletos S, Harper P. Unrepeatered DP-QPSK transmission over 352.8 km SMF using random DFB fiber laser amplification. Photonics Technology Letters. 2015;**27**(11):1041-1135

[18] Rosa P, Rizzelli G, Tan M, Harper P, Ania-Castañón JD. Characterisation of random DFB Raman laser amplifier for WDM transmission. Optics Express. 2015;**23**:28634-28639

[19] Rosa P, Le ST, Rizzelli G, Tan M, Ania-Castañón JD. Signal power asymmetry optimisation for optical phase conjugation using Raman amplification. Optics Express. 2015;**23**:31772-31778

[20] Ohki Y, Hayamizu N, Irino S, Shimizu H, Yoshida J, Tsukiji N. Pump laser module for co-propagating Raman amplifier. Furukawa Review. 2003;**24**:6-12

[21] Bromage J, Bouteiller J-C, Thiele HJ, Brar K, Nelson LE, Stulz S, Headley C, Boneck R, Kim J, Klein A, Baynham G, Jorgensen LV, Gruner-Nielsen L, Lingle RL, DiGiovanni DJ. WDM transmission over multiple long spans with bidirectional Raman pumping. Journal of Lightwave Technology. 2004;**22**(1):225-232

[22] Churkin DV, Babin SA, El-Taher AE, Harper P, Kablukov SI, Karalekas V, Ania-Castañón JD, Podivilov EV, Turitsyn SK. Raman fiber lasers with a random distributed feedback based on Rayleigh scattering. Physics Reviews A. 2010;**82**:033828

[23] Tan M, Rosa P, Iqbal MdA, Phillips ID, Nuno J, Ania-Castanon JD, Harper P. RIN mitigation in second-order pumped Raman fibre laser based amplification. In: ACP 2015, Paper. AM2E.6

[24] Phillips I, Tan M, Stephens MF, McCarthy M, Giacoumidis E, Sygletos S, Rosa P, Fabbri S, Le ST, Kanesan T, Turitsyn SK, Doran NJ, Harper P, Ellis AD. Exceeding the nonlinear-shannon limit using raman laser based amplification and optical phase conjugation. In: Optical Fiber Communication Conference, OSA Technical Digest (online) (Optical Society of America, 2014), Paper M3C.1

[25] Ellis AD, Tan M, Iqbal MA, Al-Khateeb MAZ, Gordienko V, Saavedra Mondaca G, Fabbri S, Stephens MFC, McCarthy ME, Perentos A, Phillips ID, Lavery D, Liga G, Maher R, Harper P, Doran N, Turitsyn SK, Sygletos S, Bayvel P. 4 Tb/s transmission reach enhancement using 10 × 400 Gb/s super-channels and polarization insensitive dual band optical phase conjugation. Journal of Lightwave Technology. 2016;**34**:1717-1723

[26] Churkin DV, Sugavanam S, Vatnik ID, Wang Z, Podivilov EV, Babin SA, Rao Y, Turitsyn SK. Recent advances in fundamentals and applications of random fiber lasers. Advances in Optics and Photonics. 2015;**7**:516-569

[27] Chang D, Pelouch WS, Burtesv S, Perrier P, Fevrier H. Unrepeatered high-speed transmission systems. In: Optical Fiber Communication Conference, OSA Technical Digest (Online) (Optical Society of America, 2015), Paper. W4E.3

[28] Rosa P. Quasi-lossless data tranmission with ultra-long Raman fibre laser based amplification [PhD thesis]. Aston University. 2013

[29] Cheng J, Tang M, Lau APT, Lu C, Wang L, Dong Z, Bilal SM, Fu S, Shum PP, Liu D. Pump RIN-induced impairments in unrepeatered transmission systems using distributed Raman amplifier. Optics Express. 2015;**23**(9):11838-11854

[30] Alcon-Camas M, Ania-Castañón JD. RIN transfer in 2nd-order distributed amplification with ultralong fiber lasers. Optics Express. 2010;**18**(23):23569-23575